RED PHOTOLUMINESCENCE SPECTRUM OF CuAlS$_2$: Mn

K. Sato,* M. Morita,† S. Okamoto,† S. Morita,‡ T. Kambara,‡
K. I. Gondaira‡ and H. Takenoshita§

*Tokyo University of Agriculture and Technology, Koganei, Tokyo 184, Japan
†NHK Broadcasting Research Laboratories, Setagaya, Tokyo 157, Japan
‡University of Electrocommunications, Chofu, Tokyo 182, Japan
§University of Osaka Prefecture, Sakai, Osaka 591, Japan

ABSTRACT

Photoluminescence (PL) spectra have been measured on single crystals of CuAlS$_2$ doped with manganese ions. The spectra showed a red luminescence band with a peak around 625 nm. Excitation spectrum for the 625 nm PL band and optical absorption spectrum have also been measured, in which we find peaks similar to those reported on the absorption spectrum of ZnS:Mn. These peaks can be assigned to the transitions between the multiplets of Mn ion in the tetrahedral ligand coordination and have been analyzed in the framework of the ligand-field theory. Crystal-field parameters and covalency parameters have been obtained from the analysis. Cathodeoluminescence (CL) spectra of Mn-doped CuAlS$_2$ and CuGaS$_2$ have also been studied. Red electroluminescence (EL) has also been observed in CuAlS$_2$:Mn.

KEY WORDS

CuAlS$_2$:Mn; chemical transport; photoluminescence; cathodeluminescence; electroluminescence; ligand field theory

INTRODUCTION

There have been a number of works on the electronic properties of transition metal impurities in the I-III-VI$_2$-chalcopyrite semiconductors. Full survey on this topic has been given by Schwab(1980). Concerning to Fe ions, it has been established from EPR (Schneider and coworkers, 1973), optical (Teranishi and coworkers, 1974; Sato and Teranishi, 1974) and theoretical (Kambara, 1974; Kambara and coworkers, 1975) studies that Fe ion substitutes group-III element and becomes trivalent, which introduces a strong optical absorption band in the infrared to visible region due to the charge transfer transition from 3p orbitals of ligands to the empty 3d orbitals of Fe ion. If sulfur is deficient in the chalcopyrite lattice, Fe tends to become divalent (Kaufmann, 1976). Divalent Fe does not introduce such a strong absorption band as the trivalent Fe does. For Co ion in CuGaS$_2$, it has been shown from EPR measurements that Co ion substitutes the Ga site and becomes divalent(Kaufmann and coworkers, 1974). Optical absorption spectrum of CuGaS$_2$:Co shows characteristic peaks in the visible and infrared region, which has been analyzed in terms of the ligand-field theory, from which low symmetry crystal field parameters have been deduced(Suzuki and coworkers, 1975; Sato and coworkers, 1976). It has also been observed that the optical absorption edge shifts toward lower energies, due to the incorporation of the Co ion.

As for Mn ion in the chalcopyrite semiconductors, which is the main subject of this paper, only a few papers have been published : red PL band by

Donohue and coworkers(1974) and EPR studies by Troeger and coworkers(1976). According to Donohue, $CuAlS_2$:Mn is obtained as a colorless crystal which shows red emission when excited by the mercury lamp. The EPR work by Troeger and coworkers indicates that Mn ion substitutes either Cu or Ga site in $CuGaS_2$ and that Mn at Cu site is often accompanied by a nearest neighbor Cu vacancy.

In recent years, the thin film electroluminescent(EL) devices using ZnS:Mn have been intensively studied (see for example Williams,1981). Since $CuAlS_2$ has been considered as a ternary analogue of ZnS there is a possibility of making "red" EL devices using this material. Therefore it is quite meaningful to investigate the origin of the red emission in the manganese-doped chalcopyrite semiconductor.

For this purpose we have measured photoluminescence, PL excitation and optical absorption spectra of $CuAlS_2$:Mn, from which we conclude that the red PL is caused by the recombination from the lowest excited manifold to the ground manifold of $3d^5$ electrons of Mn^{2+} ion in tetrahedral symmetry. Cathodoluminescence(CL) has also been investigated for both $CuAlS_2$:Mn and $CuGaS_2$:Mn, from which we find an emission band in $CuGaS_2$:Mn which shows no photoluminescence.
Photoacoustic spectrum was also investigated to find excited states with a non-radiative nature.

EXPERIMENTAL

Single crystals of $CuAlS_2$ doped with Mn (nominally 5 mole%) were obtained by chemical vapor transport technique using iodine as a transporting agent. Starting materials were polycrystalline powder of Cu_2S(5N) and MnS(4N), powder of S(6N), shots of Al(6N). Charges (about 5 g) were sealed in vacuo with iodine(100 mg) into fused silica ampoule with inner diameter 16 mm, the inside of which is coated by carbon.

The sealed ampoule was placed in a furnace with source temperature $850^{\circ}C$ and growth temperature $700^{\circ}C$ for two weeks. Obtained crystals were platelets with thickness about 0.5 mm and area 10 mm^2. These crystals were transparent and slightly colored pink. The dominant crystal plane determined from X-ray analyses was (112) . X-ray diffractometer measurement provided lattice constants as a=5.335 A and c=10.444 A.

Single crystals of $CuGaS_2$ doped with 5 mole% Mn have also been prepared by the same technique. Obtained crystals were colored in dark red. Lattice parameters of them were determined as a=5.348 A and c=10.469 A.

Exciting light source for PL measurement was a super-high pressure mercury lamp (150 W) with suitable pass filters to select 436 nm line. The emitted light was dispersed by a Nikon P250 grating monochromator with focal length 250 mm. The exit light was detected by a photomultiplier with a GaAs photocathode. The luminescence spectrum was corrected for the spectral response of the equipment by using a standard lamp.

Optical absorption spectrum between 0.6 eV and 3 eV was measured with a CARY 14 spectrophotometer at room temperature.

For the measurement of excitation spectrum, light from a halogen lamp dispersed by the monochromator was employed. The emitted light from the specimen was again dispersed by another monochromator and detected by the photomultiplier. PL excitation spectrum was measured with the wavelength of the second monochromator fixed at the PL peak. The obtained spectrum was corrected for the spectral dependence of the excitation light measured by using a thermopile.

CL spectra were measured by using a SEM with a suitable light collection attachment. The emitted light was dispersed by using a monochromator with a 250 mm focal length and detected by a photomultiplier with S-20 response.

Photoacoustic spectra (PAS) was measured with a specially designed cell with a microphone using a chopped light beam from a monochromator. Light source was a

100 W Xe lamp. Details have been published elsewhere (Morita,M, 1983).

We also tested whether $CuAlS_2$:Mn shows electroluminescence. Al electrode was evaporated on one side of the crystal platelet and In-Ga was painted on the opposite side. DC voltage up to 400 V was applied between the two electrodes.

EXPERIMENTAL RESULTS

Figure 1 illustrates the PL band observed in $CuAlS_2$:Mn at room temperature. Energy resolution of the measurement is about 4 meV. The spectral shape is assymmetric with a maximum at 1.96 eV and FWHM(full width at half maximum) 0.25 eV. Overall feature of the PL spectrum is quite similar to the one reported in by Donohue and coworkers(1974).
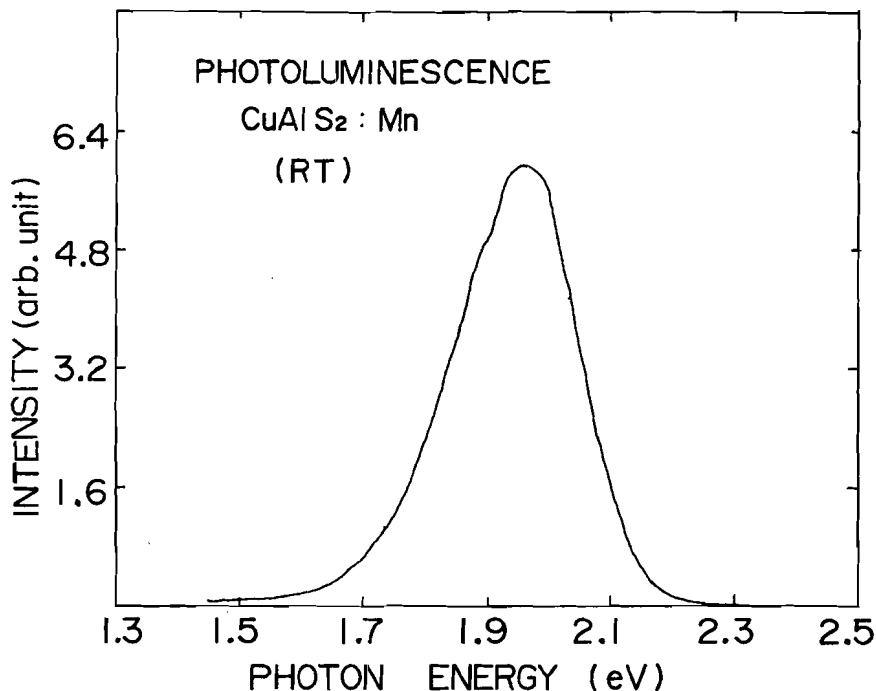

Fig. 1 Photoluminescence spectrum of $CuAlS_2$:Mn measured at room temperature. The spectrum has been corrected for the spectral response of the equipment. Excitation source is 436 nm line of a super high pressure Hg lamp.

The spectral shape does not show any substantial change when the specimen is cooled to liquid nitrogen temperature. However, at liquid helium temperature several fine structures become to be resolved as shown in Fig. 2. (Note that this spectrum has not been corrected for the spectral response of the measuring equipment.) It suggests that the total PL band consists of a number of PL lines which may be interpreted as phonon replicas of a zero-phonon line(ZPL).

Figure 3 shows the optical absorption spectrum of a single crystal of $CuAlS_2$:Mn. We find in this figure a number of absorption structures named A, B, C, D, E, and F. Recalling the studies on absorption spectra of $CuAlS_2$:Fe and $CuGaS_2$:Fe(Teranishi and coworkers, 1974; Kambara,1974) one can assign the structures A and B to the charge transfer transitions associated with Fe incorporated as trace impurities. The remainder of the absorption peaks are quite similar to those observed in ZnS:Mn(McClure, 1965), which have been interpreted as originating from the ligand-field transition between the $3d^5$
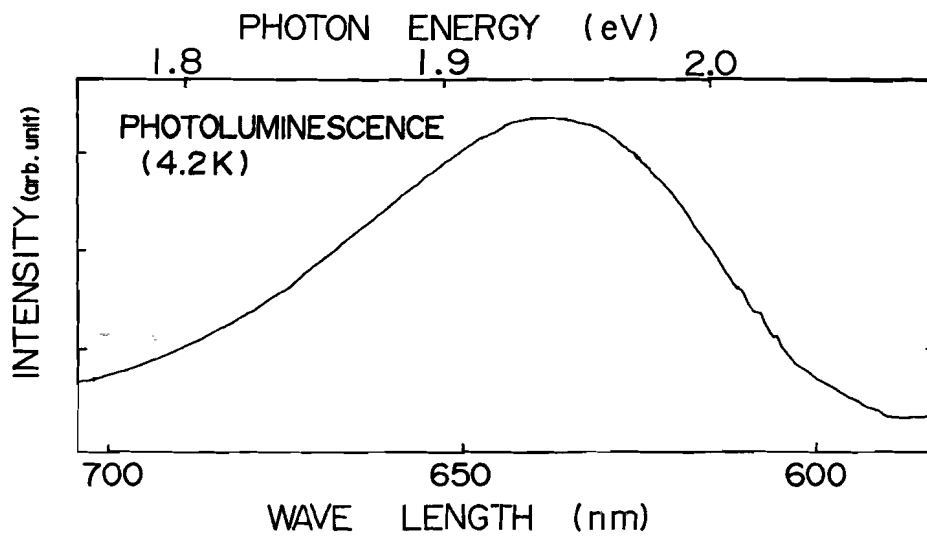
PHOTON   ENERGY   (eV)

Fig. 2 Photoluminescence spectrum of CuAlS₂ at
liquid He temperature. Correction for spectral
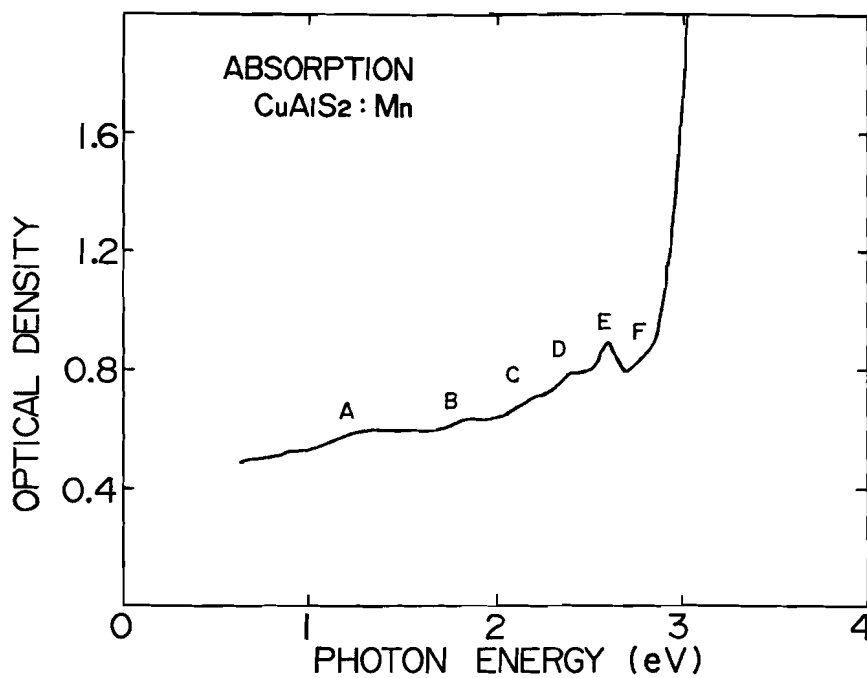dependences of equipment has not been done.

Fig. 3 Optical absorption spectrum of CuAlS₂:Mn
at room temperature measured by using a CARY 14
spectrophotometer.

transition. Details will be discussed in the next section. It should also be noted that location of the optical absorption edge of this specimen (3 eV) is much lower than that of undoped CuAlS$_2$ (3.3 eV).
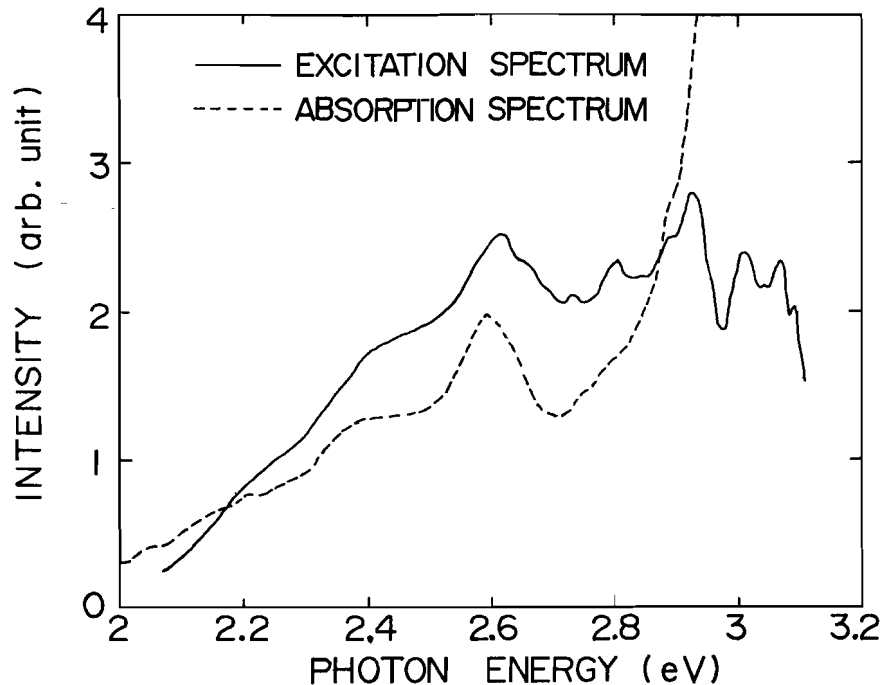

Fig.4 Excitation spectrum for 1.95 eV luminescence of   CuAlS$_2$:Mn   (solid curve).   Absorption spectrum of the same specimen is also shown by a dotted curve.
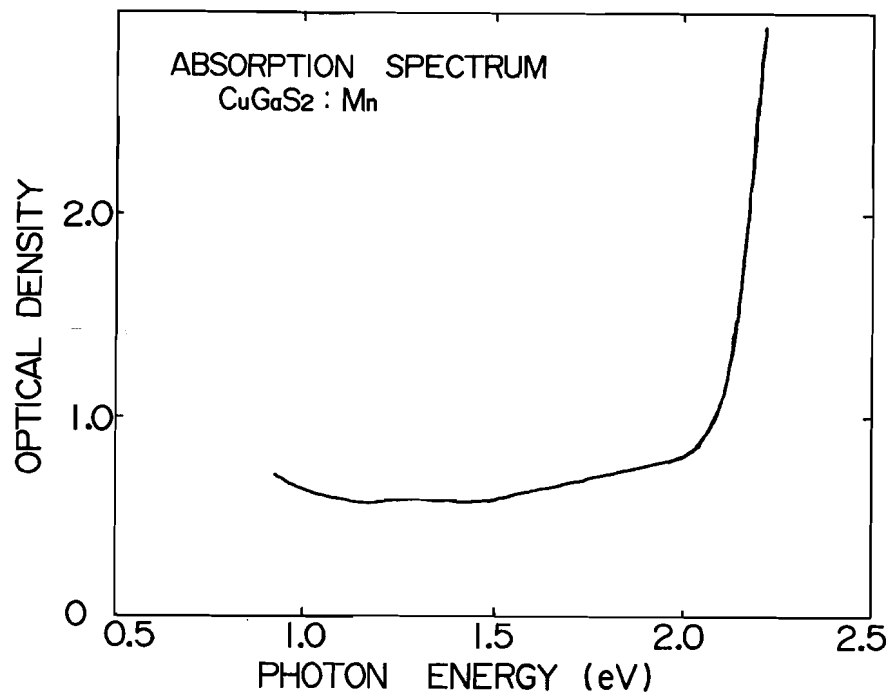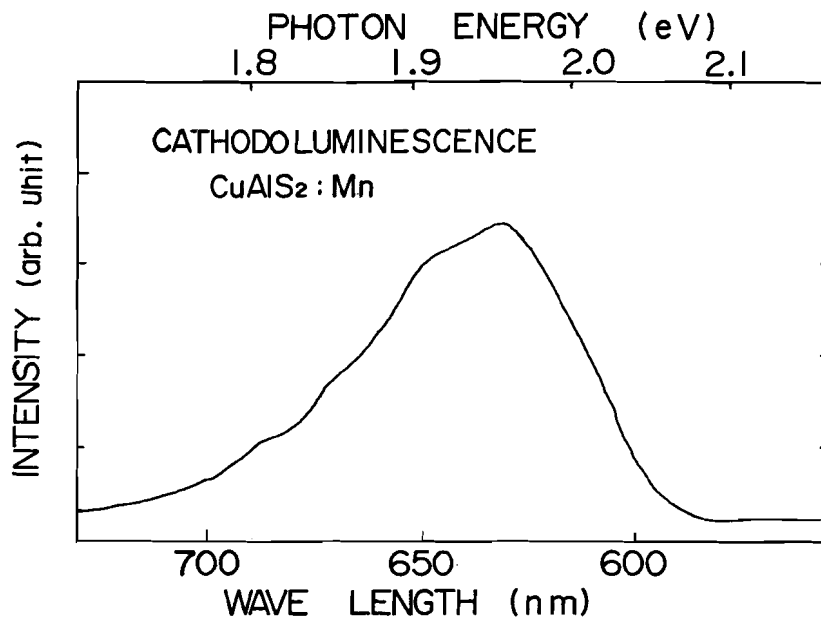
The excitation spectrum for 1.96 eV emission measured at room temperature between 2.1 eV and 3.1 eV is given by a solid curve in Fig. 4. The absorption spectrum of the same specimen for the same energy range is also given in Fig. 4 by a dotted curve. It is seen from this figure that position and shape of both curves are almost the same at least below 2.8 eV. An important point is that it is not at the absorption edge but at the absorption peaks C to F that he 1.96 eV emission is excited.

No photoluminescence was observed in CuGaS$_2$:Mn. Absorption spectrum of the same crystal is given in Fig. 5, in which no fine structures can be observed below the absorption edge. Note that the absorption edge of CuGaS$_2$:Mn is more than 0.3 eV lower than that of undoped CuGaS$_2$.
CL spectra of CuAlS$_2$:Mn and CuGaS$_2$:Mn measured at 80 K are shown in Figs. 6 and 7, respectively. These spectra have not been corrected for the spectral response of measuring instruments. The excitation beam intensity was 20 kV for CuAlS$_2$:Mn and 30 kV for CuGaS$_2$:Mn and the gain of the amplifier had to be set twice higher in the latter than in the former. Both crystals show red CL spectra. But the CL of CuGaS$_2$:Mn is weaker than that of CuAlS$_2$:Mn.
We also give a PAS spectrum of CuAlS$_2$:Mn in Fig. 8. The spectrum shows that PA signal is not strongly excited by the fine structures C to F but strongly excited by a shoulder structure coresponding to the absorption edge (3eV) which is more than 0.3 eV lower than the one of the undoped CuAlS$_2$.

Electroluminescence was observed on CuAlS$_2$:Mn crystal.Emitted light was red just like the case of PL. The threshold voltage was 150 to 200 V. Current at the threshold was 2 mA. Since sample thickness of used crystals was 0.5 mm, we do not think this voltage is discouragingly high. Thin film device would work with appropriate voltages.

ABSORPTION SPECTRUM
$CuGaS_2$: Mn

OPTICAL DENSITY

2.0

1.0

0

0.5   1.0   1.5   2.0   2.5

PHOTON ENERGY (eV)

Fig. 5 Absorption spectrum of $CuGaS_2$:Mn

PHOTON ENERGY (eV)
1.8   1.9   2.0   2.1

CATHODOLUMINESCENCE
$CuAlS_2$: Mn

INTENSITY (arb. unit)

700   650   600

WAVE LENGTH (nm)

Fig. 6 Cathodoluminescence spectrum of $CuAlS_2$:Mn measured at 80 K. Excitation beam voltage is 20 kV.

PHOTON ENERGY (eV)

1.8   1.9   2.0   2.1

CATHODOLUMINESCENCE
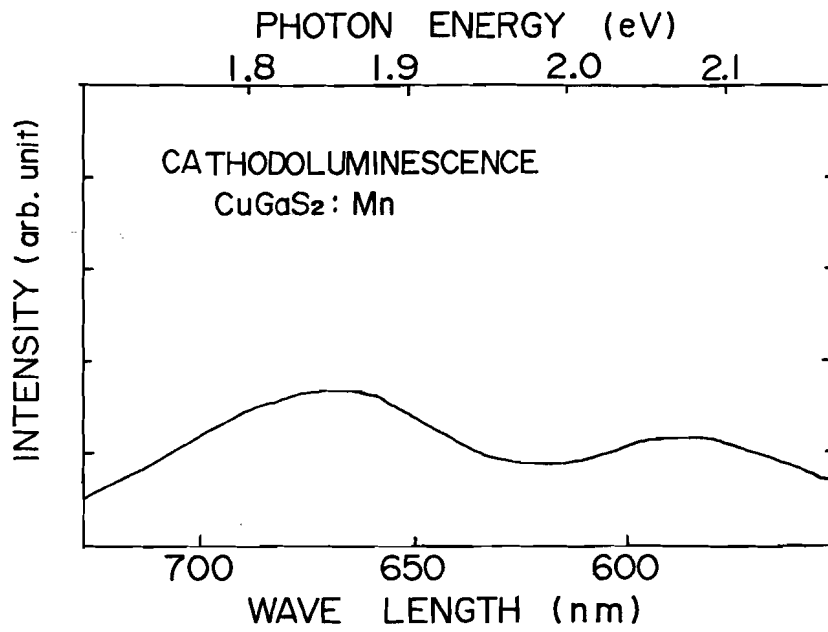
CuGaS₂ : Mn

INTENSITY (arb. unit)

700   650   600

WAVE LENGTH (nm)

Fig. 7 Cathodoluminescence spectrum of CuGaS₂:Mn measured at 80 K. Excitation beam voltage is 30 kV.

PAS SPECTRUM

CuAlS₂ : Mn

1.5

1.0

INTENSITY

0.5

0

b   c   d   e   f   g

1.5   2.0   2.5   3.0   3.5   4.0

PHOTON ENERY (eV)
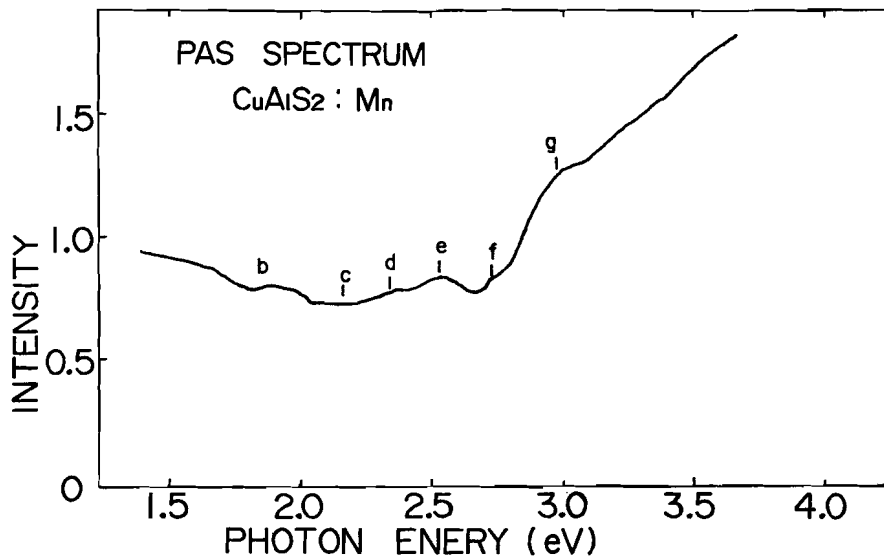
Fig. 8 Photoacoustic spectrum of CuAlS₂:Mn

DISCUSSION

First, we assume that Mn substitutes Cu site when incorporated in $CuAlS_2$ lattice. The reason for this assumption is given in the following. Since ionic radii of Cu^+, Al^{3+} and Mn^{2+} are 0.96, 0.57 and 0.91 A, respectively, substitution is easier on the Cu^+ site than on the Al^{3+} site. For $CuGaS_2$, however, EPR results indicates that Mn substitutes both Cu and Ga sites; this might be accounted for by larger ionic radius of Ga^{3+} (0.62 eV).

In addition to the argument of ionic radii, strong support for the above assumption is provided by the fact that Mn-doped $CuAlS_2$ is "colorless": Usually, crystals of $CuAlS_2$ obtained by the chemical transport are colored blue due to the strong charge transfer transition caused by unintentional Fe^{3+} impurities which substitute Al^{3+} site. When Mn^{2+} substitutes Cu^+ site, the Fe impurity at the Al site becomes divalent in order to satisfy the charge neutrality conditions. As stated in INTRODUCTION divalent Fe introduces no absorption in the photon energy region of argument, making the sample colorless.

For higher concentration of Mn as in this work, the sample becomes to show pink coloration, which is caused by the optical absorptions C to F ranging between 2 and 3 eV as shown in Fig. 3. As stated in the preceding section, the absorption peak C to F may be attributed to the optical transition between the $3d^5$-manifolds of Mn^{2+} ion in the tetrahedral coordination: Taking into account the assignment for the case of ZnS:Mn, it seems quite natural to assign the peaks C, D, E and F to transitions from the ground state ($^6A_1$) to excited states $^4T_1$, $^4T_2$, $^4A_1+^4E$ and $^4T_2$, respectively.

These transitions have been analyzed in the framework of the ligand-field theory. Most commonly accepted treatment involves three parameters Dq, B and C. Here Dq stands for the crystal field splitting parameter, while B and C for Racah's parameters. Least square fitting to the observed energies provides values for the set of parameters as follows: $Dq=578$ cm^{-1}, $B=335$ cm^{-1} and $C=3525$ cm^{-1}. Calculated energy levels are given in the second column in Table 1 together with the experimental energies in the first column. Although the fitting seems quite satisfactory, the obtained value of B is unreasonably small compared with the free ion value for Mn^{2+} (860 cm^{-1}), leading to an unusually large C/B value 10.52.

TABLE 1. Observed and calculated energy levels of Mn^{2+} in $CuAlS_2$.

Observed Energy (eV)	Calculated Energy (eV)		Assignment
	$Dq=578$ cm^{-1} $B=335$ cm^{-1} $C=3525$ cm^{-1}	$Dq=600$ cm^{-1} $N_t=0.926$ $N_e=0.966$	
C 2.21	2.18	2.06	T_1
D 2.38	2.41	2.38	T_2
E 2.59	2.60	2.57	A
E 2.59	2.60	2.51	E
F 2.78	2.75	2.96	T_2
	2.89	3.26	E
	3.65	3.29	T_1
	3.97	3.36	A
	4.08	4.22	T_1
	4.31	4.63	T_2

Another choice of fitting parameters have been tried: We leave Racah's parameters B and C unchanged from their free ion values ($B=860$ cm^{-1} and $C=3850$ cm^{-1}); instead, we introduce normalizing factors N_t and N_e to account for the effect of covalent bonding, as given by Curie and coworkers (1974). Physically, parameters N_t and N_e represent reduction of electronic interactions for t_2 and e orbitals, respectively. The values of parameters which gives the best fit to the experimental values are $Dq=600$ cm^{-1}, $N_t=0.926$ and $N_e=0.966$. Since it can be assumed that deviation of N from unity corresponds to the degree of covalency, it may be easily understood that N_t

takes smaller value than N_e in tetrahedral coordination. However, as seen in the third column in Table 1 agreement of calculated energies with the experimental values are rather unsatisfactory. Such disagreement is not serious since we have neglected in the present treatment any other perturbations such as low-symmetry crystal field, spin-orbit interaction and dynamic Jahn-Teller effect.

We also carried out similar calculations to get parameters for ZnS:Mn. They are listed in Table 2 together with those for CuAlS₂:Mn. Inspite of poor fitting the N_t and N_e provides better physical insights to the problem of covalency. By comparing the values of N_t and N_e for CuAlS₂:Mn with those for ZnS:Mn we find that Dq is much larger and N_t is much smaller in CuAlS₂:Mn than in ZnS:Mn. It suggests that Mn^{2+} ion suffers larger effect of covalency in chalcopyrite than in zincblende.

TABLE 2. Two sets of parameters for Mn^{2+} in zincblende and chalcopyrite crystals. (cm^{-1})

Material	Dq	B	C	Dq	N_t	N_e
ZnS:Mn	545	499	3302	478	0.941	0.952
CuAlS₂:Mn	578	335	3525	600	0.926	0.966

Anyway, from theoretical analyses we have come to the conclusion that the absorption structures named C, D, E and F seen in Fig. 2 are interpreted in terms of the ligand field transitions in the Mn^{2+} ion.

In the next place, it has become clear from comparison between the absorption and PL excitation spectra that the red PL band is excited by the optical transitions between the multiplets associated with $3d^5$ electrons of Mn^{2+} ion. Therefore, it is quite reasonable to assign the red emission band to the transition from the lowest excited state $^4T_1$ to the ground state $^6A_1$.

As stated in EXPERIMENTAL RESULTS the PL band can be interpreted as the multiphonon sideband attached to the zero phonon luminescence line (ZPL). Two fine structures are clearly resolved in 4.2 K PL spectrum shown in Fig. 2; their energies are 2.046 eV and 2.039 eV. Infrared absorption spectrum (Koschel and his coworkers, 1973) locates TO-phonon lines at 214 cm^{-1} (26.5 meV), 262 cm^{-1} (32.4 meV), 432 cm^{-1} (53.6 meV) and 450 cm^{-1} (55.8 meV). Taking into account the energy separation (7 meV) of observed fine structures we assign them to phonon sideband accompanied by emission of 214 cm^{-1} and 262 cm^{-1} phonons, from which position of ZPL is located at 2.07 eV. This value is very close to the energy 2.08 eV estimated for ZPL by taking the mean value of absorption peak (2.2 eV) and emission peak (1.96 eV).

In the next place, we discuss why CuGaS₂:Mn shows no photoluminescence while it shows cathodoluminescence. It may be assumed that the energy positions of excited levels of Mn^{2+} in CuGaS₂ is not so different from those in CuAlS₂:Mn, since the CL peak of the former is only slightly (0.1 eV) different from that of the latter. On the other hand, absorption edge of CuGaS₂:Mn is located around 2.2 eV, which is much lower than that of CuAlS₂:Mn (3 eV); excited levels of Mn^{2+} is completely masked by the strong absorption.
Absorption edges of Mn-doped chalcopyrites are more than 0.3 eV lower than those of undoped crystals: such apparent shift of absorption edge is commonly seen in chalcopyrites with divalent impurities and may be attributed to defect states introduced to keep charge neutrality in the crystal. Such defect states have tendencies to become non-radiative recombination centers. This story is supported by the photoacoustic spectrum of CuAlS₂:Mn. Small peaks named c, d, e and f are clearly corresponding to Mn^{2+} excitation, while a strong shoulder g at 3 eV may be connected with the defect level just below the true absorption edge (3.4 eV) of this crystal. Since larger PAS signal corresponds to stronger non-radiative recombination, the experimental result means PL is quenched by the defect levels.
Although PAS of CuGaS₂:Mn has not been measured, it is quite probable that the lack of PL is caused by the non-radiative nature of the defect levels just below the absorption edge, which mask the excited levels of Mn^{2+} completely.

The illumination by the 436 nm Hg line cannot excite the Mn levels efficiently but excite the defect center which brings about the apparent absorption edge, where non-radiative recombination occurs.
Electron beams, on the other hand, can excite the localized Mn center directly by the impact excitation. This is why we can observe cathodoluminescence in $CuGaS_2$:Mn crystals.

CONCLUSION

In the first place, we have observed red PL, CL and EL in $CuAlS_2$:Mn, the peak energy being 1.96 eV. The red PL band is excited by the optical absorptions associated with the $3d^5$ manifolds of Mn^{2+} ion; from which the red emission band is assigned to the multiphonon sideband attached to the radiative recombination from the lowest excited state $^4T_1$ to the ground state $^6A_1$. The position of ZPL is estimated as 2.07 eV.
Next, the absorpion structures of $CuAlS_2$ have been interpreted in terms of the ligand field theory. Two sets of parameters were obtained, which give the best fit to the experimental energies as follows: one set being $Dq=578$ cm^{-1}, $B=335$ cm^{-1} and $C=3525$ cm^{-1}, and the other $Dq=600$ cm^{-1}, $N_t=0.926$ and $N_e=0.966$ The latter parameters lead to conclusion that covalency is stronger $CuAlS_2$:Mn than in ZnS:Mn.
In the last, The reason why $CuGaS_2$:Mn shows no PL was discussed in terms of the crystalline defect introduced to maintain the charge neutrality, which becomes the non-radiative recombination center.

REFERENCES

Curie, D., C. Barthou, and B. Canny (1974). J. Chem. Phys., 61, 3048-3062.
Donohue, P. C., J. D. Bierlein, J. E. Hanson, and H. S. Jarrett (1974). J. Electrochem. Soc., 121, 829-832.
Kambara, T. (1974). J. Phys. Soc. Japan, 36, 1625-1635.
Kambara, T., K. Suzuki, and K.I. Gondaira (1975). J. Phys. Soc. Japan, 39, 764-771.
Kaufmann, U., A. Rauber, and J. Schneider (1974). Solid State Commun., 15, 1881-1884.
Kaufmann, U. (1976). Solid State Commun., 19, 213-215.
Koschel, W.H., V. Hohler, A. Rauber, and J. Baars (1973). Solid State Commun., 13, 1011-1016.
McClure, D. S. (1963). J. Chem. Phys. 39, 2850-2855.
Morita, M. and F. Sato (1983). Japan. J. Appl. Phys. 22, suppl. 22-3, 199-20
Sato, K., and T. Teranishi (1974). J. Phys. Soc. Japan, 37, 415-422.
Sato, K., T. Kawakami, T. Teranishi, T. Kambara, and K. I. Gondaira (1976). J. Phys. Soc. Japan, 41, 937-941.
Schneider, J., A. Rauber, and G. Brandt (1973). J. Phys. Chem. Solids, 34, 443-450.
Schwab, C. (1980). Japan. J. Appl. Phys., 19, suppl. 19-3, 59-66.
Suzuki, K., T. Kambara, K. I. Gondaira, K. Sato, K. Kondo, and T. Teranishi (1975). J. Phys. Soc. Japan, 39, 1310-1315.
Teranishi, T., K. Sato, and K. Kondo (1974). J. Phys. Soc. Japan, 36, 1618-1624.
Troeger, G.L., R. N. Rogers, and H. M. Kasper (1976). J. Phys. C, 9, L73-L78.
Williams, F. (1981). J. Luminescence, 23, 1-16.